THE JOURNAL OF BIOLOGICAL CHEMISTRY VOL. 286, NO. 1, pp. 594–606, January 7, 2011

Function of Partially Duplicated Human α7 Nicotinic Receptor Subunit *CHRFAM7A* Gene

*POTENTIAL IMPLICATIONS FOR THE CHOLINERGIC ANTI-INFLAMMATORY RESPONSE**

Received for publication, August 30, 2010, and in revised form, October 18, 2010 Published, JBC Papers in Press, November 3, 2010, DOI 10.1074/jbc.M110.180067

Ana M. de Lucas-Cerrillo[‡1], M. Constanza Maldifassi[‡2], Francisco Arnalich[§], Jaime Renart[¶], Gema Atienza[‡], Rocío Serantes[‡§], Jesús Cruces[¶‖], Aurora Sánchez-Pacheco[¶‖], Eva Andrés-Mateos[**], and Carmen Montiel[‡3]

From the Departamentos de [‡]Farmacología y Terapéutica, [§]Medicina Interna, y [‖]Bioquímica, Universidad Autónoma de Madrid, Facultad de Medicina/Hospital La Paz, IdiPAZ, Arzobispo Morcillo 4, 28029 Madrid, Spain, the [¶]Instituto de Investigaciones Biomédicas "Alberto Sols," Consejo Superior de Investigaciones Científicas, Arturo Duperier 4, 28029 Madrid, Spain, and the [**]McKusick-Nathans Institute of Genetic Medicine, The Johns Hopkins University School of Medicine, Baltimore, Maryland 21205

The neuronal α7 nicotinic receptor subunit gene (*CHRNA7*) is partially duplicated in the human genome forming a hybrid gene (*CHRFAM7A*) with the novel *FAM7A* gene. The hybrid gene transcript, dupα7, has been identified in brain, immune cells, and the HL-60 cell line, although its translation and function are still unknown. In this study, dupα7 cDNA has been cloned and expressed in GH4C1 cells and *Xenopus* oocytes to study the pattern and functional role of the expressed protein. Our results reveal that dupα7 transcript was natively translated in HL-60 cells and heterologously expressed in GH4C1 cells and oocytes. Injection of dupα7 mRNA into oocytes failed to generate functional receptors, but when co-injected with α7 mRNA at α7/dupα7 ratios of 5:1, 2:1, 1:1, 1:5, and 1:10, it reduced the nicotine-elicited α7 current generated in control oocytes (α7 alone) by 26, 53, 75, 93, and 94%, respectively. This effect is mainly due to a reduction in the number of functional α7 receptors reaching the oocyte membrane, as deduced from α-bungarotoxin binding and fluorescent confocal assays. Two additional findings open the possibility that the dominant negative effect of dupα7 on α7 receptor activity observed *in vitro* could be extrapolated to *in vivo* situations. (i) Compared with α7 mRNA, basal dupα7 mRNA levels are substantial in human cerebral cortex and higher in macrophages. (ii) dupα7 mRNA levels in macrophages are down-regulated by IL-1β, LPS, and nicotine. Thus, dupα7 could modulate α7 receptor-mediated synaptic transmission and cholinergic anti-inflammatory response.

Neuronal α7 nicotinic acetylcholine receptors (α7 nAChRs)[4] are widely expressed in the central and peripheral nervous systems. In neurons, homomeric α7 nAChRs, composed of five α7 subunits, modulate neurotransmitter release in presynaptic nerve terminals and induce excitatory impulses in postsynaptic neurons (1–4). Signaling through α7 nAChRs in the central nervous system has been associated with neuronal plasticity and cell survival (5–7), although impaired activity of this receptor has been implicated in the pathogenesis of schizophrenia, Alzheimer disease, and depression (8–12). The presence of α7 nAChRs has also been reported in non-neuronal cells such as vascular and brain endothelial cells, bronchial epithelial cells, keratinocytes, astrocytes, synoviocytes, thymocytes, lymphocytes, bone marrow cells, monocytes, macrophages, microglia, and astrocytes (see Ref. 13 and the references therein). Interestingly, the α7 nAChR expressed in macrophages (and probably in other immune cells) is essential for vagus nerve regulation of acute pro-inflammatory cytokine release during systemic inflammatory response (see Ref. 14 and references therein). The α7 nAChR is a target for natural and synthetic ligands; however, little is known about endogenous receptor-regulating molecules.

The α7 nicotinic subunit encoded by gene *CHRNA7* is located on the long arm of chromosome 15 (15q13-q14). A hybrid gene (*CHRFAM7A*) resulting from a fusion of a partial duplication of *CHRNA7* with *FAM7A* gene was identified at 1.6 Mb from *CHRNA7* toward the centromeric region (15, 16). *CHRNA7* and *CHRFAM7A* are highly homologous (>99%) from exon 5 to the 3′-UTR region. In contrast, the hybrid has replaced exons 1–4 of the original *CHRNA7* with the exons D, C, B, and A of *FAM7A*, inserted in an Alu sequence of intron 4 of *CHRNA7*, 700 bp upstream from exon 5. Moreover, *CHRFAM7A* is polymorphic with a few rare individuals who completely lack a copy of the gene. Most people (>95%) have one or two *CHRFAM7A* copies, and in some cases, there is a 2-bp deletion in exon 6 (16, 17). The acquisition of this duplication seems to be a recent evolutionary event because *CHRFAM7A* only appears in humans and not in other higher primates (18). The above findings would indicate that the hybrid gene could confer an evolutionary advantage on the genotype with the duplication.

* This work was supported by Grant SAF2008-05347 (to C. M. and F. A.) from the Ministerio de Ciencia y Tecnología and Fundación Mutua Madrileña, Spain.

[1] Recipient of fellowship from Programa de Formación de Personal Investigador (Ministerio de Ciencia e Innovacion, Spain).

[2] Recipient of fellowship from Beca Chile (CONICYT, Ministerio de Educación, Chile.

[3] To whom correspondence should be addressed. Tel.: 34-91-4975390; Fax: 34-91-4975353; E-mail: carmen.montiel@uam.es.

[4] The abbreviations used are: nAChR, neuronal nicotinic acetylcholine receptor; ACh, acetylcholine; αBgtx, α-bungarotoxin; CTX, cerebral cortex; ER, endoplasmic reticulum; 5HI, 5-hydroxyindole; I_{ACh}, ACh-elicited current; I_{Nic}, nicotine-elicited current; MØ, macrophages differentiated from monocytes; PBMC, peripheral blood mononuclear cells; ROI, region of interest; Q-PCR, real time quantitative PCR; TBP, TATA-binding protein; ANOVA, analysis of variance.

To date, the possible functional significance of this *CHRNA7* duplication is unknown, although there are conflicting reports in the literature suggesting an association between *CHRFAM7A* polymorphisms and certain psychiatric and neurological disorders, such as schizophrenia, bipolar depression, Alzheimer disease, dementia with Lewy bodies, or Pick disease (19–24). The *CHRFAM7A* transcript, dupα7, has been identified in hippocampus, cortex, corpus callosum, thalamus, putamen, caudate nucleus, and cerebellum (15, 25–26) and in peripheral blood mononuclear cells (PBMC), lymphocytes, synoviocytes, as well as HL-60 cells (25–28). Despite its wide distribution, to date there is no experimental evidence demonstrating that this transcript is translated and what the possible functional role of the resulting protein might be.

This study seeks to shed some light on the last two questions. Using GH4C1 cells and oocytes, we have studied the function of heterologously expressed dupα7 protein, and, to study the native transcript, we use HL-60 cells, human CTX, and human macrophages. A set of experimental approaches, including molecular biology and confocal images of labeled receptors, combined with pharmacological and electrophysiological techniques, has been used throughout this study.

EXPERIMENTAL PROCEDURES

Cell Lines and Oocytes—The rat pituitary-derived GH4C1 cells were grown in DMEM containing 10% fetal calf serum, and the human acute promyeloid leukemic HL-60 cell line in RPMI 1640 medium supplemented with 10% fetal bovine serum. In both cases, 100 units·ml^{-1} of penicillin G sodium and 100 μg·ml^{-1} of streptomycin sulfate were added. Both cell types were maintained at a density of 1×10^6 to 2×10^6 cells/ml at 37 °C in a humidified 5% CO_2 atmosphere. Mature female *Xenopus laevis* frogs were obtained from a commercial supplier (*Xenopus* Express, Haute-Loire, France). Techniques for oocyte isolation have been described by our group previously (29–32).

Isolation of Human Monocytes and Differentiation to Macrophages—The PBMCs were isolated from blood buffy coats from healthy individual donors, and the monocyte-enriched cell population was then purified from PBMC by a double density gradient protocol as described previously (33). Monocytes were collected, washed, resuspended in complete RPMI 1640 medium, and seeded either onto coverslips in 24-well tissue culture plates (5×10^5 cells per well) or onto 60-mm Petri dishes (10^6 cells·ml^{-1}). Cells were allowed to differentiate to macrophages (MØ) for 7–9 days in the presence of macrophage colony-stimulating factor (2 ng·ml^{-1}) in complete culture medium.

Cloning of dupα7 cDNA— dupα7 was cloned in two steps, using either human thalamus (for the 3′-region) or MØ (for the 5′-region) RNAs. After first strand cDNA synthesis with M-MLV reverse transcriptase (Invitrogen), the 3′-region was amplified with primers A7S4 (5′-CACACACGTCTCGCCCTCGCCCTGCTGGT-3′) and A7AS4 (5′-CACCCCCAAATCTCGCCAA-3′). We amplified the 5′-region with primers DUPA7S (5′-TGACAATCCAAAGGTGCACA-3′) and A7AS3 (5′-CACACACGTCTCGAGGGCGGAGATGAGCA-3′). Both fragments were cloned in pMOS-Blue. To obtain the whole coding sequence, the 3′-region fragment was digested with BsmBI (underlined in primers A7S4 and A7AS3) and SacI and ligated to the vector containing the 5′-region, digested with the same enzymes. The complete cDNA was transferred directly from dupα7·pMOS-Blue to pcDNA3 (digested with XbaI and BamHI). For oocyte injection experiments, dupα7 was amplified from dupα7·pMOS-Blue with DupSpeI(S) 5′-ACTAGTGCCACCATGCAAAAATATTGCATCTACC-3′ and DupNotI(AS) 5′-GCGGCCGCCGTGGTTACGCAAAGTCTTTGG-3′ (with the recognition sequences for SpeI and NotI underlined, respectively) and cloned into pSP64T digested with the same enzymes.

Preparation of RNAs—Techniques for RNA isolation from cells and tissues and *in vitro* transcription mRNA synthesis have been described elsewhere (31, 32). Plasmids dupα7·pSP64T, α7·pSP64T, and RIC3·pGEMH19 were linearized with BamHI, Xba, and NheI, respectively, and then transcribed *in vitro* with SP6 (dupα7, α7) or T7 (RIC3) polymerases using the mMACHINE kit from Ambion (Austin, TX). Messenger RNA was dissolved in RNase-free water (1 μg/μl), and aliquots were stored at −80 °C until used.

Immunofluorescent Staining and Confocal Microscopy—GH4C1 cells were electroporated with plasmids dupα7·pcDNA3, α7·pcDNA3, or pcDNA3. They were then plated on 12-mm glass coverslips for 48 h before processing. Cells were fixed with 4% paraformaldehyde, permeabilized with 0.25% Triton X-100, and stained overnight with the monoclonal anti-α7 subunit antibody (Mab306, Sigma, 1:3000) in PBS with 5% normal goat serum at 4 °C, followed by incubation with AlexaFluor 488 goat anti-mouse IgG (1:400) for 2 h at room temperature. All images were captured with a Leica TCS SP2 spectral confocal laser scanning microscope as reported previously (31, 32). Fluorescence intensity, expressed as arbitrary units, was measured in a narrow region of interest (ROI) located between the plasma membrane and the cell nucleus. In other cases, fluorescence intensity was measured along the *x* axis of the entire cell body.

Techniques for mRNA injection and immunodetection of foreign proteins expressed in intact injected oocytes have been described elsewhere (31, 32). Five days after injection, protein expression was analyzed using the same antibodies and dilutions as for GH4C1 cells. Oocytes were mounted in glycerol/buffer (70:30) under a glass coverslip on a glass dual-well slide. The slide was fastened upside down on the stage of the Leica confocal microscope and visualized with a ×20 lens. The fluorescent signal was determined as arbitrary units in an ROI located on the surface of the animal pole of the oocyte.

α-Bungarotoxin Staining and Confocal Microscopy—Native expression levels of functional α7 nAChRs in MØ were analyzed using fluorescein isothiocyanate-labeled α-bungarotoxin (FITC-αBgtx) and confocal microscopy. Cells were incubated with FITC-αBgtx (3μg·ml^{-1}; Sigma) as described previously (34). Cells from the same culture incubated with nicotine (500 μM) or αBgtx (1 μM), before and during the addition of FITC-αBgtx, were used as a negative control. After several rinses, MØ were fixed in 4% paraformaldehyde, washed, and mounted on coverslips. Heterologous expression of functional α7 nAChRs in mRNA-injected oocytes was ana-

lyzed 5 days after injection by incubation with FITC-αBgtx (3 $\mu g \cdot ml^{-1}$) in Barth's solution, as has been described for MØ. Oocytes were rinsed, fixed in 4% paraformaldehyde, mounted in glycerol/buffer (70:30), and visualized by confocal microscopy. Fluorescent signal was determined as described elsewhere (31, 32).

Electrophysiological Recordings and Surface Receptor Binding Assay—Electrophysiological recordings of foreign proteins expressed in oocytes have been described in detail by our group elsewhere (29, 32, 35). The agonist concentration eliciting half-maximal current (EC_{50}) and the Hill coefficient values were estimated through nonlinear regression analysis using the four-parameter logistic equation of the GraphPad Prism software. Total surface expression of αBgtx-binding sites on the surface of mRNA-injected oocytes was assayed with ^{125}I-α Bgtx (Amersham Biosciences), as described elsewhere (36). Briefly, 5 days after injection, oocytes placed on 24-well plates were preincubated for 15 min with Ringer's solution containing fetal calf serum (6%). Then they were incubated for 2 h at 18 °C in a final volume of 300 μl of the above solution containing increasing concentrations (1–10 nM) of ^{125}I-α Bgtx. After incubation, labeled medium was removed and oocytes washed several times with Ringer's solution before counting total bound radioactivity in a Beckman Coulter γ counter. Nonspecific binding was determined in noninjected oocytes incubated under the same conditions; this value was subtracted from total binding to yield specific binding.

Northern Blot Analysis—Poly(A)$^+$ RNAs (4 μg/lane) isolated from human CTX and from HL-60 cells were separated by 1% formaldehyde/agarose gel electrophoresis, transferred onto a nylon blotting membrane (Schleicher & Schuell), and hybridized at 68 °C overnight with the ^{32}P-labeled probe (781 bp) obtained by digestion of dupα7·pMOS-Blue with SpeI and SmaI. The resulting fragment starts in the ATG of exon B and extends to the 51st nucleotide of exon 10; thus, it recognizes the dupα7 and α7 transcripts.

Isolation of Polysome-bound mRNA and Real Time Quantitative PCR (Q-PCR)—Polysome-bound mRNA from HL-60 cells was obtained as described by del Prete *et al.* (37), except that cells were pretreated with 0.1 $mg \cdot ml^{-1}$ cycloheximide for 10 min at 37 °C. In the conditions used, ribonucleoprotein particles, isolated ribosomal subunits, and monosomes remain in fractions 1–10 (from the top) whereas polysomes are recovered in fractions 11–20. After this, monosomic and polysome fractions were regrouped into two pools, and 1 aliquot (10 μl, diluted to 100 $ng \cdot \mu l^{-1}$) from each pool was used for Q-PCR mRNA quantification. We added 10 ng of *in vitro* transcribed luciferase mRNA (from pGL3-control plasmid) to each aliquot as an endogenous marker for quantification. The level of gene expression in human CTX and human MØ was also assessed by Q-PCR for reverse-transcribed mRNA or total RNA, respectively. A combination of TaqMan and SYBR Green-based assays for amplicon detection on the ABI Prism 7900 device was used. The following primers were used: for dupα7, forward 5′-CAATTGCTAATCCAGCATTTGT-3′ (position 603–624 of sequence in NM_139320) and reverse 5′-CCCAGAAGAATTCACCAACACG-3′ (position 704–683 in NM_139320); for α7, Hs_CHRNA7_2_SG, QuantiTech Primer Assay, QT01681211 (Qiagen); for TBP (encoding for the TATA-binding protein), forward 5′-CGGTTTGCTGCGGTAATCA-3′ and reverse 5′-TGTTGGTGGGTGAGCACAAG-3′; for luciferase, forward 5′-TGGAAGACGCCAAAAACATAAAG-3′ and reverse 5′-AGCAATTGTTCCAGGAACCAGGGC-3′. For dupα7 and α7 mRNA quantification in MØ, TaqMan Hs00415199_m1 and Hs01063372_m1 (Applied Biosystems) were used, respectively. Analysis of the melting curves demonstrated that each pair of primers amplified a single product. Q-PCR for each mRNA was performed in triplicate, and all results were normalized to the expression of 18 S rRNA (Ambion primers). Relative gene expression values were calculated by the comparative Δ*Ct* method using the Sequence Detection System 1.2 software (Applied Biosystems).

Chemicals—Unless otherwise indicated, all products were purchased from Sigma. AlexaFluor 488 goat anti-mouse IgG was from Molecular Probes (Eugene, OR), and DMEM and RPMI media were from Invitrogen. The human recombinant IL-1β was purchased from PeproTech (London, UK), and PNU120596 was from Tocris Bioscience (Bristol, UK).

RESULTS

Analysis of the dupα7 Coding Sequence—The cloned full-length dupα7 cDNA codes for a 1236-nucleotide sequence similar to the one previously deposited in NCBI and that corresponds to the dupα7 isoform 1 (accession number NM_139320) with minimal variations. Our sequence contains two neutral transitions, C/T and A/G at positions 654 and 986, respectively, but it retains the two TG nucleotides at positions 497–498 on exon 6. Using the ConPred II software for transmembrane topology prediction, one can observe that the resulting 412-amino acid polypeptide preserves many of the distinctive features of the nAChR subunits, with the N and C termini outside the membrane and the four transmembrane domains (M1–M4) as well as the long intracellular loop between M3 and M4 (Fig. 2*A*). However, as has been reported previously (15), dupα7 protein does lose a substantial part of the long N-terminal domain of α7 and thus lacks the recognition sites for ACh and α Bgtx.

Heterologous Expression of dupα7 Versus α7—Expression of foreign proteins was analyzed in GH4C1 cells transfected with plasmids dupα7·pcDNA3 or α7·pcDNA3 and in oocytes injected with dupα7 and α7 mRNAs. The GH4C1 cell line was selected for two reason. 1) It does not express dupα7 or α7, making visualization of foreign protein expression feasible. 2) It expresses the RIC-3 chaperone (38) making it an excellent model to express functional α7 nAChRs. The confocal images obtained in transfected GH4C1 cells stained with Mab306 show a high expression level of both proteins, in contrast to low fluorescence detected in the negative control cells transfected with pcDNA3 (Fig. 1, *A* and *C*). The analysis of the protein expression along the *x* axis of the cell reveals two expression peaks located in the cell periphery; the α7 peak seems to be located more externally than the dupα7 peak (Fig. 1*B*).

Noninjected oocytes (control) have low basal fluorescence, which increases markedly at or near the cell surface of the

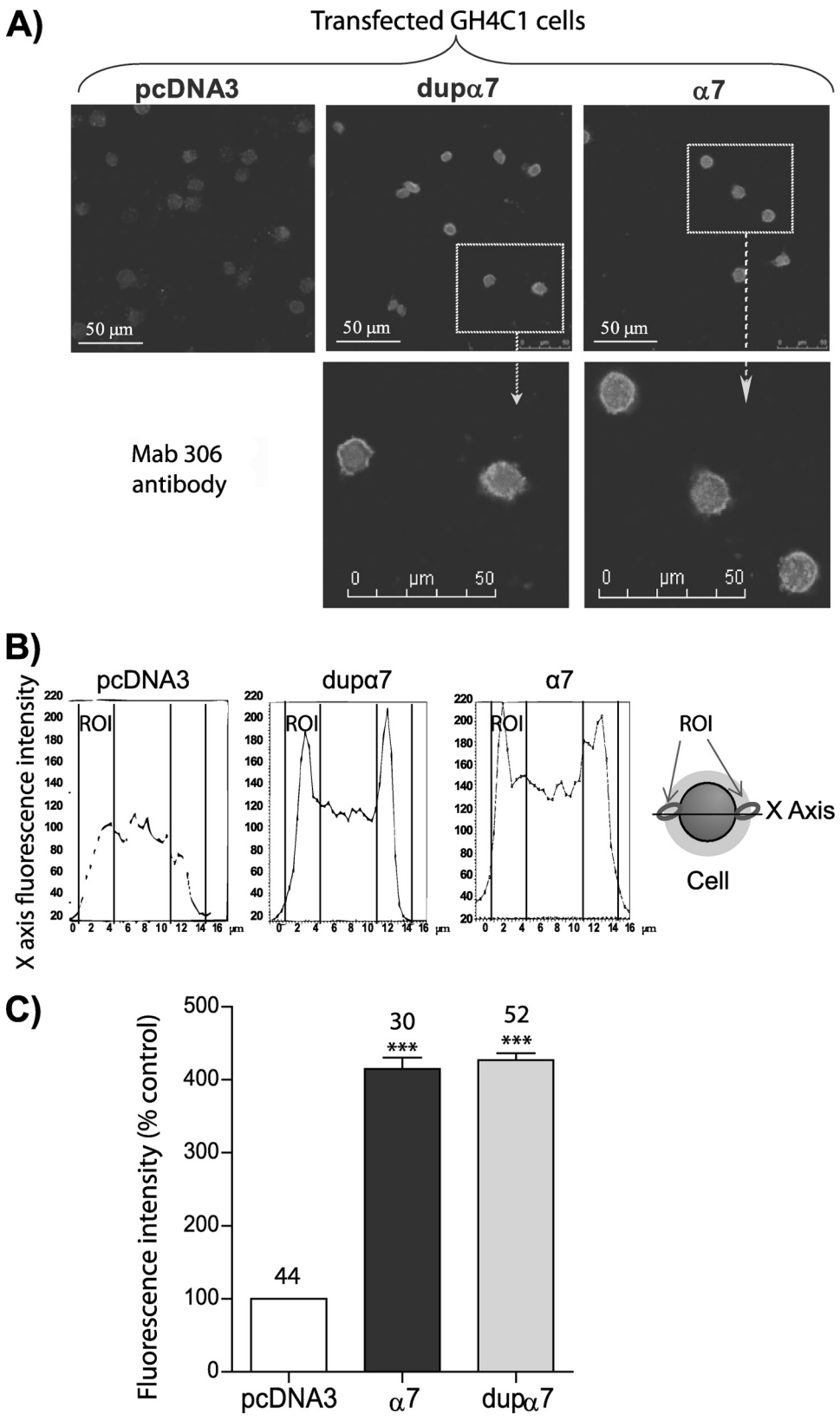

FIGURE 1. **Expression of dupα7 and α7 subunits in GH4C1 cells.** *A*, confocal images showing the fluorescent signal generated in transfected GH4C1 cells stained with the Mab306 antibody. *B,* scanned fluorescence intensity along the *x* axis in three typical cells of the images above. *C*, *histogram* shows pooled results of fluorescence intensity measured in the region of interest (*ROI*) indicated in *B*. Each *bar* represents the mean ± S.E., expressed as a percentage of control (transfected with pcDNA3), in the number of cells shown at the *top*. At least four to six different coverslips from two independent cell cultures were used for each experimental condition. Data were analyzed using ANOVA and Bonferroni post hoc tests; ***, $p \leq 0.001$ upon comparing transfected *versus* control cells.

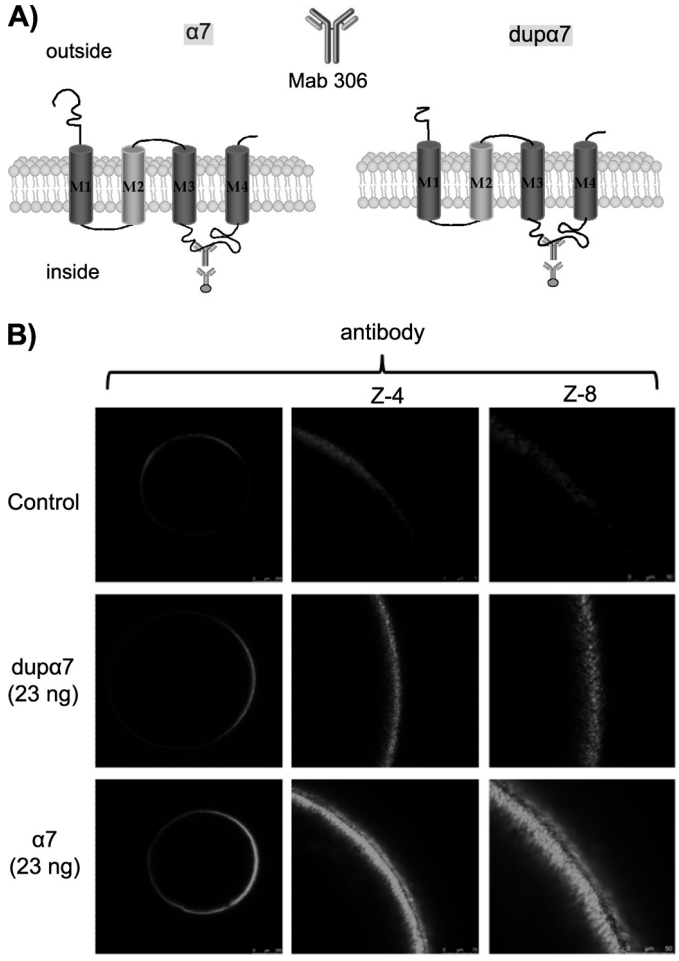

FIGURE 2. **Confocal images of oocytes expressing dupα7 and α7 subunits.** *A*, diagram of tertiary structures of α7 and dupα7 proteins; the Mab306 antibody binding region is also indicated. *B*, *left column* shows overall confocal (Z-scan) images of three typical intact oocytes (out of five), noninjected (*control*), or injected with dupα7 or α7 mRNA and immunostained with the antibody. *Central* and *right columns* show, at a higher magnification, the fluorescent signal at the animal surface in the three oocytes.

animal hemisphere in dupα7 or α7 mRNA-injected oocytes incubated with the above antibody (Fig. 2*B*). Nevertheless, the fluorescence signal corresponding to dupα7 is significantly lower (33 ± 7%, $n = 7$; $p \leq 0.05$) than that found in α7 mRNA-injected oocytes. As has been reported previously, no intracellular fluorescence was observed in mRNA-injected oocytes under any experimental condition (39). This may be due to the following: 1) the inability of the laser to penetrate far into a large 1-mm cell; 2) the quenching of the fluorescent signal by the oocyte yolk/pigment; or 3) the possibility that intracellular antibody distribution may be too diffuse to be detected.

Dominant Negative Effect of dupα7 on α7 Currents Expressed in Oocytes—Once the heterologous expression of the dupα7 protein in GH4C1 cells and oocytes was confirmed, we proceeded to study its possible functional role in the latter cell type. The study began with the electrophysiological recording of ACh-elicited currents (I_{ACh}) in oocytes injected with α7 mRNA (2.5 ng/oocyte). In all experiments RIC3 mRNA (2.5 ng) was co-injected with α7 mRNA because this treatment almost doubles the amplitude and reproducibility of the recorded currents. Repeated pulses of ACh (100 μM, 1 s) or nicotine (30 μM, 1 s) at 1-min intervals, applied to oocytes injected with increasing concentrations of dupα7 mRNA (from 0.5 to 25 ng/oocyte), failed to produce any response (not shown). In contrast, co-injection of dupα7 with α7 mRNA (2.5 ng) resulted in a concentration-dependent reduction of α7 current induced by nicotine (I_{Nic}) (Fig. 3, *A* and *B*). The co-injection of 0.5 ng/oocyte of dupα7 mRNA (α7/dupα7 ratio of 5:1) was sufficient to reduce significantly (26 ± 8%, $n = 6$; $p \leq 0.01$) the amplitude of I_{Nic}, and this blockade exceeded 90% when the α7/dupα7 ratio was 1:5 or 1:10.

The next experiments were designed to analyze the nature of the dominant negative effect of dupα7 on the α7 current. One possibility is that dupα7 is integrated into the pentameric structure of the expressed receptor, changing its pharmacological properties. Another possibility is that dupα7 interferes with the proper assembly of α7 subunits that form mature homopentameric α7 nAChR, which is essential for receptor trafficking from endoplasmic reticulum (ER) to the cell membrane. The following experiments sought to explore both possibilities.

dupα7 Reduces α7 Current Amplitude but Not Receptor Response to ACh—Fig. 3 (*C* and *D*) shows the concentration-response curves to ACh in oocytes injected with 2.5 ng of α7 mRNA and the corresponding amount of dupα7 mRNA according to the indicated α7/dupα7 ratio. Each oocyte was stimulated with successive pulses of increasing concentrations of agonist and, at the end of experiment, with a control pulse of 1 mM ACh that induced the maximum current (I_{max}). Fig. 3*C* shows the original traces of I_{ACh} obtained in one α7 mRNA-injected oocyte stimulated as described above. As expected, for a given ACh concentration, the higher the proportion of dupα7 in the mixture of injected mRNA, the lower the I_{ACh}. Thus, the I_{max} for the combinations 1:0, 2:1, 1:1, and 1:5 of α7/dupα7 was 8.4 ± 1.5, 3.9 ± 0.7, 2.1 ± 0.5, and 0.6 ± 0.2 μA, respectively. The currents induced by each of the ACh concentrations tested in the oocyte were normalized to the I_{max}. Fig. 3*D* shows pooled results of normalized currents obtained in several oocytes ($n = 5–6$) assayed for each condition; each value represents mean ± S.E. The EC_{50} and Hill coefficient values are shown in the table below; the analysis of variance (ANOVA) applied to both parameters showed no significant differences between the four groups of oocytes.

dupα7 Reduces the Number of Functional α7 nAChRs in the Oocyte Membrane—To examine whether the dupα7 effect was due to a reduction in the number of functional α7 nAChRs incorporated into the surface of the oocyte, we incubated the oocytes with either the Mab306 antibody, which detects both α7 and dupα7, or with FITC-αBgtx, which binds to the extracellular N-terminal region present in the α7 subunit alone. Three groups of mRNA-injected oocytes (α7, dupα7, or 1:1 α7/dupα7), along with a fourth group without an injection (control) were analyzed. The confocal images in Fig. 4*A* show the fluorescent signal detected in eight typical intact oocytes from the same donor subjected to one or the other staining process. Fig. 4*B* shows the average fluorescence values, expressed as a percentage of the control, determined in several oocytes ($n = 5–8$) used for testing each experimen-

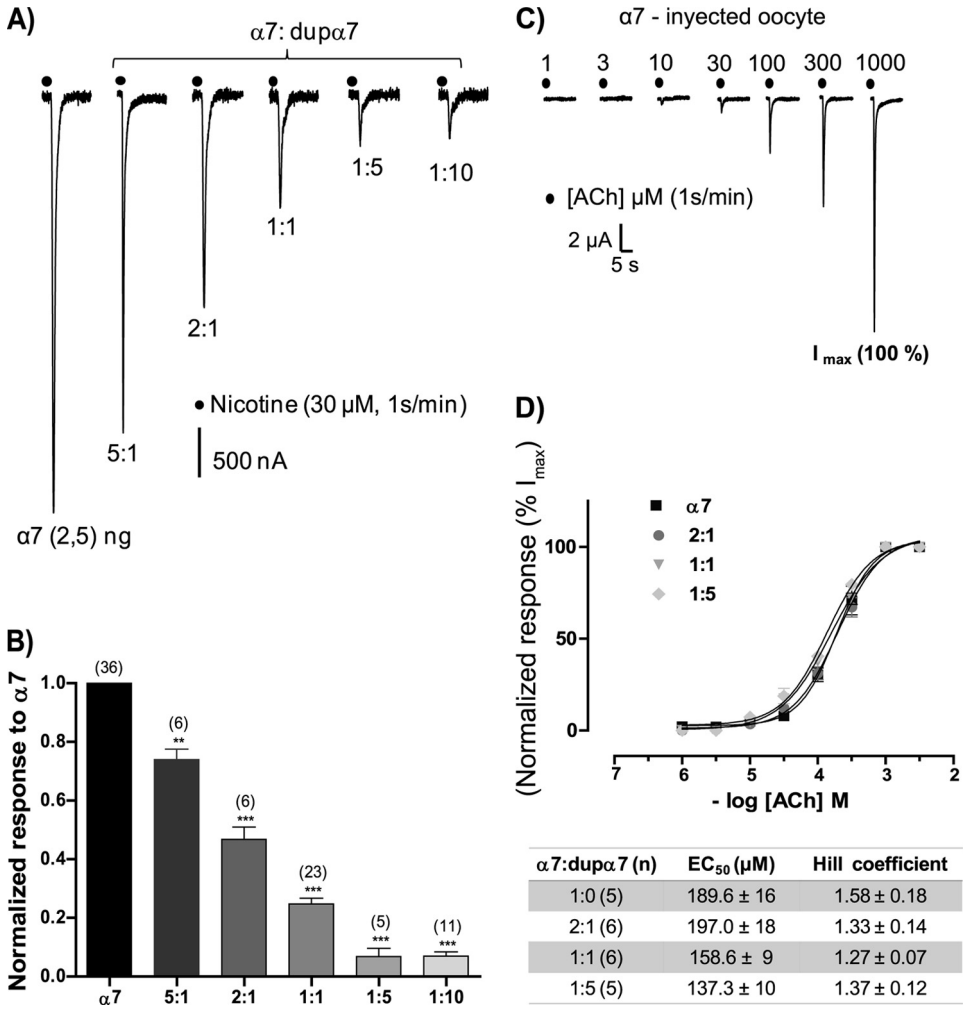

α7:dupα7 (n)	EC_{50} (μM)	Hill coefficient
1:0 (5)	189.6 ± 16	1.58 ± 0.18
2:1 (6)	197.0 ± 18	1.33 ± 0.14
1:1 (6)	158.6 ± 9	1.27 ± 0.07
1:5 (5)	137.3 ± 10	1.37 ± 0.12

FIGURE 3. **dupα7 produces a dominant negative effect on α7 currents without affecting receptor response to ACh.** In all combinations assaying α7/dupα7 mRNAs, the amount of injected α7 mRNA (2.5 ng/oocyte) remained constant. *A,* original traces of inward nicotine-elicited currents (I_{Nic}) in six oocytes injected with different combinations of α7/dupα7 mRNAs. Each oocyte was voltage-clamped at −70 mV and stimulated with repeated pulses of nicotine; the original traces correspond to the time when I_{Nic} becomes stabilized. *B,* diagram showing the I_{Nic} amplitude values for each α7/dupα7 combination normalized to α7 mRNA-injected oocytes. Each *bar* shows the mean ± S.E. of the number of oocytes in *parentheses*. The data were analyzed using ANOVA and Dunnett post hoc tests to compare all groups with the α7-mRNA injected group; **, $p \leq 0.01$ and ***, $p \leq 0.001$. *C,* original traces of inward currents (I_{ACh}) induced by increasing concentrations of ACh applied as successive pulses in one α7 mRNA-injected oocyte; finally, a control pulse of 1 mM ACh to generate a maximum current (I_{max}) was applied. *D,* dependence of I_{ACh} amplitude, normalized to I_{max}, on the concentration of ACh assayed in oocytes injected with different combinations of α7/dupα7 mRNAs; values are mean ± S.E. of the number of oocytes shown in *parentheses* in the *table* below. The *table* also shows mean ± S.E. of EC_{50} and Hill coefficient values obtained for each combination tested. Analysis of variance showed no significant differences among the four groups of oocytes analyzed.

tal condition. Although the antibody detected a robust expression of α7 nAChRs and a small fluorescent signal generated by dupα7 in oocytes injected with one or the other mRNA, FITC-αBgtx only detected the expression of the first protein. However, regardless of the staining technique used, the co-injection of dupα7 with α7 mRNA significantly reduced the expression of α7 nAChRs on the surface of the oocyte. In fact, in oocytes labeled with FITC-αBgtx, the α7 signal was reduced (≈70%) to levels that were indistinguishable from those in the control. It should be noted that, regardless of the staining process used, confocal images show a polarized distribution of nicotinic subunits on the animal membrane of the oocyte.

Co-expression of dupα7 with α7 Reduces the Number of ^{125}I-α Bgtx-binding Sites on the Oocyte Surface—Two groups of oocytes injected with α7 mRNA (control) or with the combination 1:4 of α7/dupα7 mRNA were incubated with increasing concentrations of ^{125}I-α Bgtx as described under "Experimental Procedures." Compared with controls, the injection of dupα7 mRNA reduced markedly and significantly the maximum specific binding of radioligand (B_{max}), from 8,277 ± 331 to 4,552 ± 288 cpm; $p \leq 0.01$ (Fig. 4*C*, *bottom panel*). Additionally, the equilibrium dissociation constant (K_d) suffered a slight but significant increase in the presence of dupα7 (from 1.37 ± 0.17 to 4.28 ± 0.56 nM; $p \leq 0.05$).

Effect of Positive Allosteric Modulators on I_{ACh} Expressed in Oocytes Injected with Several Combinations of α7/dupα7 mRNA—The following experiments were designed to look for possible pharmacological differences among oocytes injected with different α7/dupα7 mRNA ratios. We used two positive allosteric modulators of α7 nAChRs, each one representative of one of the two available allosteric groups. Group I includes

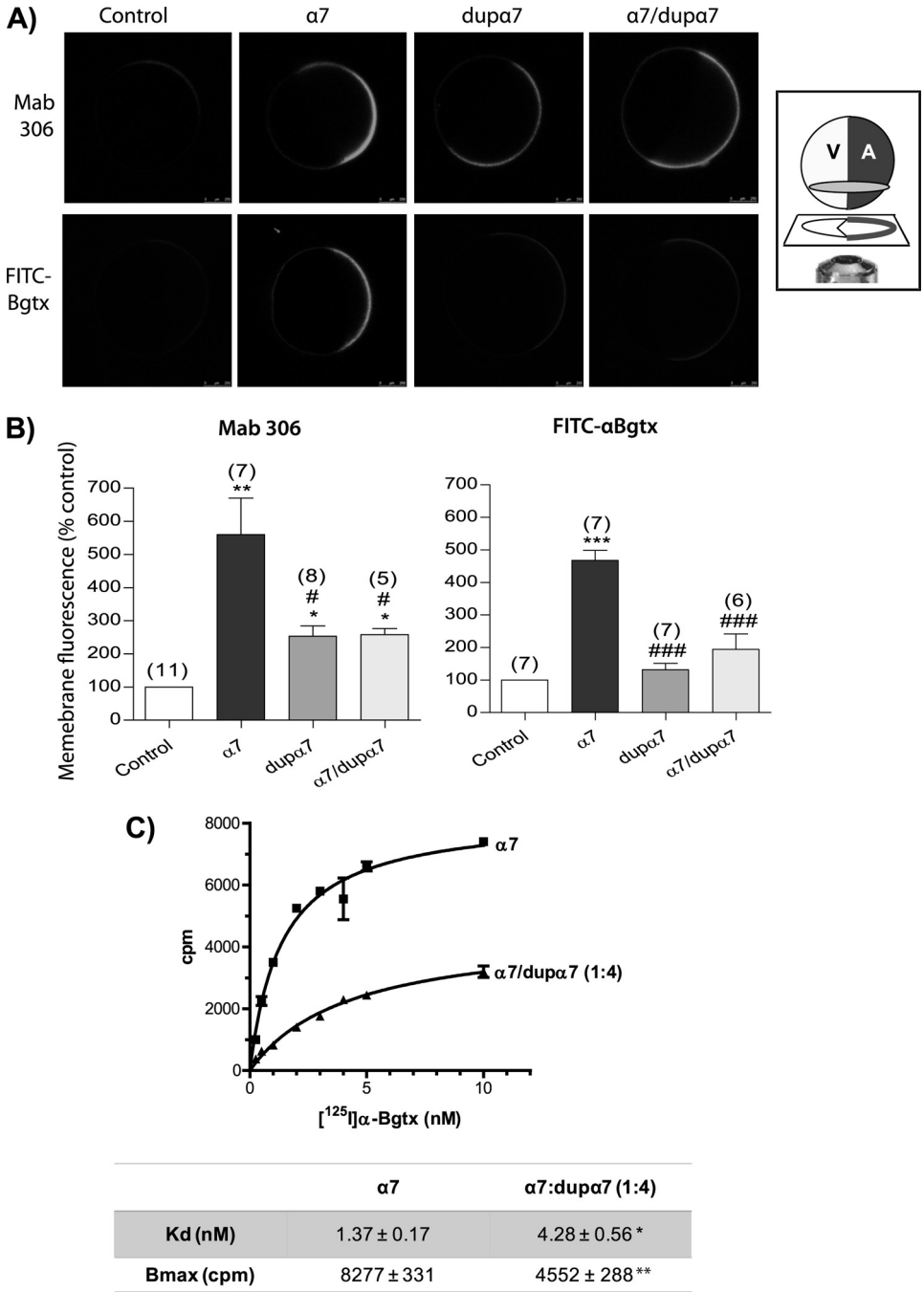

	α7	α7:dupα7 (1:4)
Kd (nM)	1.37 ± 0.17	4.28 ± 0.56 *
Bmax (cpm)	8277 ± 331	4552 ± 288 **

FIGURE 4. **dupα7 reduces the number of functional α7 nAChRs expressed on the oocyte surface.** *A*, representative confocal images of eight intact oocytes labeled with Mab306 antibody (*top row*) or FITC-αBgtx (*bottom row*). Oocytes were injected with α7 (20 ng), dupα7 (20 ng), or with the combination (1:1) of α7/dupα7 mRNAs; on the *left* are two control noninjected oocytes. *Inset,* oocyte orientation on the confocal microscope stage; *V* and *A* indicate the vegetal and animal hemisphere, respectively. *B*, histograms show pooled results of fluorescent intensity determined in an ROI located on the animal surface of the oocyte; data were normalized in respect to control. Each *bar* shows the mean ± S.E. of the number of oocytes in *parentheses*. The data were analyzed by ANOVA; *, $p \leq 0.05$; **, $p \leq 0.01$; ***, $p \leq 0.001$ upon comparing injected with control oocytes. #, $p \leq 0.05$, and ###, $p \leq 0.001$ after comparing oocytes injected with dupα7 or α7/dupα7 mRNAs *versus* α7-mRNA-injected oocytes. *C,* saturation curves showing specific binding of ^{125}I-α Bgtx to the surface of intact oocytes injected with α7 mRNA (20 ng) or with the combination α7/dupα7 (20:80 ng). The adjustment of the curves and the determination of K_d and B_{max} values were done with GraphPad Prism5 software. The analysis of the variation in K_d and B_{max} values between the two groups of oocytes was performed with the Mann Whitney test for analysis of two nonparametric variables, *, $p \leq 0.05$; **, $p \leq 0.01$. A total of 6–8 oocytes from two different donors were used for each value plotted in the curves.

agents like 5-hydroxyindole (5HI), which potentiates the peak agonist-evoked response mediated by α7 nAChR, but it does not modify the duration of the response (40). Meanwhile, PNU120596, representative of group II, increases the peak agonist-evoked response and markedly prolongs the macroscopic currents in the presence of agonist, possibly by interfering with the desensitization process (41). The different effects of these two groups of positive allosteric modulators indicate the existence of distinct allosteric binding sites with specificity for either 5HI or PNU120596.

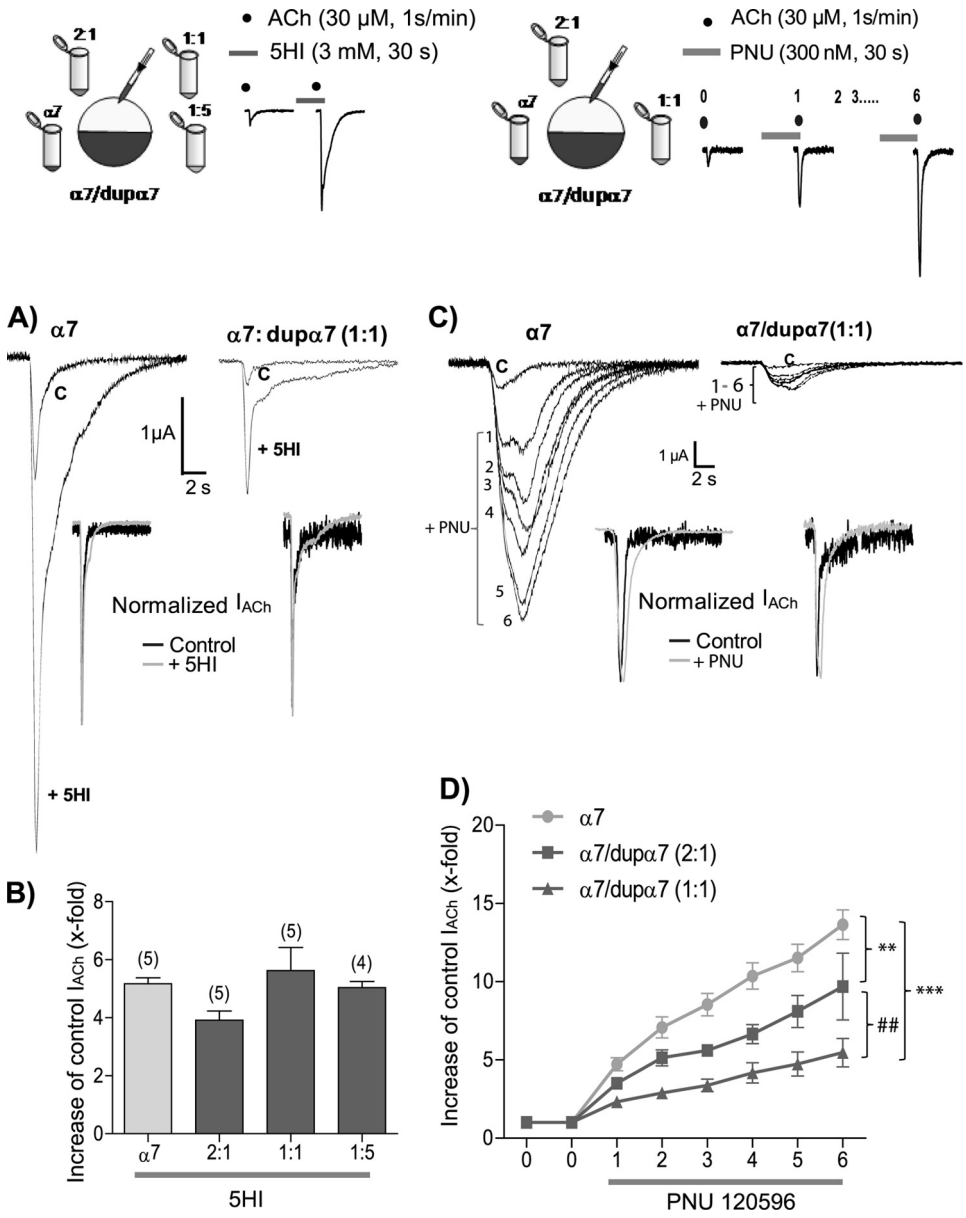

FIGURE 5. **Positive allosteric modulator PNU120596, but not 5-hydroxyindole, can distinguish among oocytes injected with different combinations of α7/dupα7 mRNAs.** The tested combinations and the experimental design are shown at the *top*. The α7 mRNA (2.5 ng/oocyte) remains constant in all combinations. Oocytes, voltage-clamped at −70 mV, were stimulated with regular pulses of ACh in the absence or presence of the modulator. The effect of 5HI was evaluated on a single ACh pulse, although in the case of PNU120596 (*PNU*), the oocyte was stimulated with an initial pulse of ACh (0 = control) followed by six successive ACh pulses in the presence of the modulator. *A,* original traces of ACh-elicited currents (I_{ACh}), in the absence or presence of 5HI, obtained in two mRNA-injected oocytes. The left and right records correspond to one α7-mRNA and one α7/dupα7-mRNA (1:1)-injected oocyte, respectively. *Inset,* normalized currents of both oocytes. *B,* histogram shows the number of times that 5HI increases the control peak I_{ACh} in each group of oocytes. Each *bar* shows the mean ± S.E. of the number of oocytes in *parentheses*. Analysis of variance and Dunnett post hoc tests showed no differences between groups of oocytes. *C,* original traces showing the PNU120596 effect on I_{ACh} over the 1st to 6th pulses of ACh in two mRNA-injected oocytes. The left and right records correspond to one α7-mRNA and one α7/dupα7-mRNA (1:1) injected oocyte, respectively. *Inset,* normalized currents obtained in both oocytes corresponding to the initial (control) and the 3rd pulse of ACh in the presence of PNU. *D, graph* representing the number of times that P PNU120596 increased the control peak I_{ACh} during the six pulses in each group of oocytes. Each point represents the mean ± S.E. of seven oocytes per group. Data were analyzed using ANOVA and Bonferroni post hoc tests. **, $p \leq 0.01$; ***, $p \leq 0.001$; ##, $p \leq 0.01$ after the comparison of the different oocyte groups as indicated.

The effects of 5HI on I_{ACh} were analyzed in several groups of oocytes injected with different combinations of α7/dupα7 mRNA, using the group of α7 mRNA-injected oocytes as reference (Fig. 5, *upper left panel*). The oocytes were stimulated with successive pulses of ACh (30 μM, 1 s), applied at intervals of 1 min. Once the I_{ACh} was stable (control), we incubated the oocytes with 3 mM 5HI (30 s before and during the ACh pulse), evaluating its enhancing effect on control I_{ACh}. Fig. 5 (*A* and *B*) shows that 5HI increased the amplitude of control I_{ACh} about 5-fold and that this effect was not significantly different in any oocyte group. Additionally, 5HI did not alter the kinetics of I_{ACh} in any of the oocyte groups as can be deduced after normalization of the original traces obtained in two oocytes injected with either α7 or α7/dupα7 (1:1) mRNAs (Fig. 5*A*, *inset*).

A different design was used to evaluate the effect of PNU120596 in oocytes injected with several combinations of α7/dupα7 mRNA (Fig. 5, *top right panel*). The α7 mRNA-injected group was used as reference. The oocytes were stimulated with successive pulses of ACh (30 μM, 1 s, at 1-min intervals). Once I_{ACh} was stabilized (control), we perfused 300 nM PNU120596 before and during the ACh pulse, evaluating its enhancing effect on control I_{ACh}. Because there was a progressive positive effect of the modulator on I_{ACh} over successive ACh pulses, we evaluated this effect over six consecutive agonist pulses. Fig. 5 (*C* and *D*) shows that the higher the proportion of dupα7 in the mixture of injected mRNA, the lower the enhancing effect of PNU120596 on peak I_{ACh}. Normalization of the currents (Fig. 5*C*, *inset*) shows that the allosteric modulator delays desensitization of I_{ACh} in all the oocyte groups, with no significant differences, probably because of the shortness of the ACh pulse.

Identification of the dupα7 Transcript in Cerebral Cortex and HL-60 Cells—Although the presence of the dupα7 transcript has been detected in different brain areas, immune cell types, and the HL-60 cell line by PCR, the size of this mRNA is unknown. Northern blot analysis was performed with mRNAs extracted from human CTX and HL-60 cells because the latter cell type mainly expresses dupα7 and not α7 (25). Fig. 6*A* shows a well defined band of ≈3.9 kb in HL-60 cells, also present in CTX, the latter also containing bands of 5.8, 3.3, 2.1, and 1.4 kb.

dupα7 mRNA Is Translated in HL-60 Cells—Antibodies that specifically differentiate α7 and dupα7 are not available, so it is still impossible to demonstrate the existence of dupα7 protein *in vitro* or *in vivo*. To solve this difficulty, we have gone a step backwards in the translation process and used an indirect approach, one that looks for dupα7 mRNA in the polysomal fraction because we know that polysome-bound mRNAs are being translated (42, 43). After sucrose gradient centrifugation of an HL-60 cell extract as described under "Experimental Procedures," a bioanalysis assay for each fraction showed that tRNA appears in fractions 1–4, the migration peak for the small 40 S ribosomal subunit (18 S peak) is in fractions 5–6, followed by the migration peak for the large 60 S ribosomal subunit (28 S peak) in fractions 7–10, whereas fractions 11–20 contain the polysomal fraction (28 S and 18 S). All fractions were regrouped into two pools (monosomal and polysomal) as described under "Experimental Procedures." Relative expression of dupα7, TBP, and luciferase mRNAs was quantified in the two pools. TBP mRNA was used as the positive control because it is constitutively translated in all cell types and therefore must be present in the "polysomal fraction" of HL-60 cells. Fig. 6*B* shows the relative levels of TBP mRNA and dupα7 mRNA in monosomal and polysomal pools, expressed as a percentage of the total mRNA in both fractions. The results reveal that, as expected, the TBP transcript was in the heavy sucrose fractions (polysomes), as was the dupα7 transcript.

Levels of the dupα7 Transcript in Human Cerebral Cortex and Macrophages and Its Modulation by Different Treatments—We performed Q-PCR experiments to determine levels of dupα7 and α7 mRNAs in CTX and MØ. The

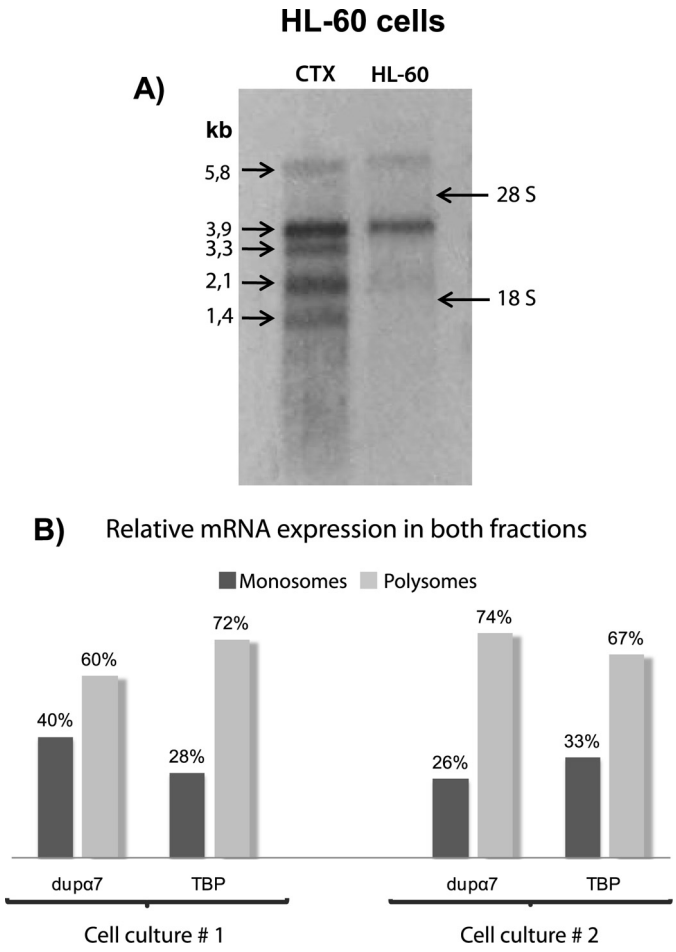

FIGURE 6. **Determination of the size and relative expression levels of dupα7 mRNA in the monosomal and polysomal fractions of HL-60 cells.** *A,* Northern blot performed with RNAs from human CTX and HL-60 cells showing the 3.9-kb transcript in both lanes and different α7 transcript of 5.8, 3.3, 2.1, and 1.4 kb in CTX. *B,* levels of dupα7 or TBP mRNAs in monosomal and polysomal fractions of HL-60 cells quantified by Q-PCR. The results are expressed as a percentage of each messenger in the two fractions. Values were obtained in triplicate and correspond to two different cultures of HL-60 cells subjected to ultracentrifugation on a sucrose gradient as described under "Experimental Procedures."

PCR was performed with human CTX mRNA or with total RNA from cultured human MØ using the primers listed under "Experimental Procedures." The results in Fig. 7*A* show that dupα7 expression is around 22% of the α7 expression in CTX. The opposite happens in MØ, where the α7 mRNA levels are ~7% of those of dupα7. Despite this low level of α7 mRNA in relation to dupα7 in MØ, these cells clearly show the expression of functional α7 nAChRs, as reflected by confocal images of MØ in FITC-αBgtx-labeled cultures (Fig. 7*B*, *left panel*). The receptor specificity of this staining is demonstrated by the disappearance of the fluorescent signal in cells preincubated with 1 μM αBgtx or 500 μM nicotine (Fig. 7*B*, *right panel*). Finally, MØ in culture were subjected to different treatments to evaluate if dupα7 mRNA levels could be modulated. Fig. 7*C* shows that the pro-inflammatory cytokine interleukin-1β (IL-1β), LPS from *Salmonella abortus* and nicotine, all markedly and significantly reduced dupα7 mRNA expression in MØ cultures (Fig. 7*C*).

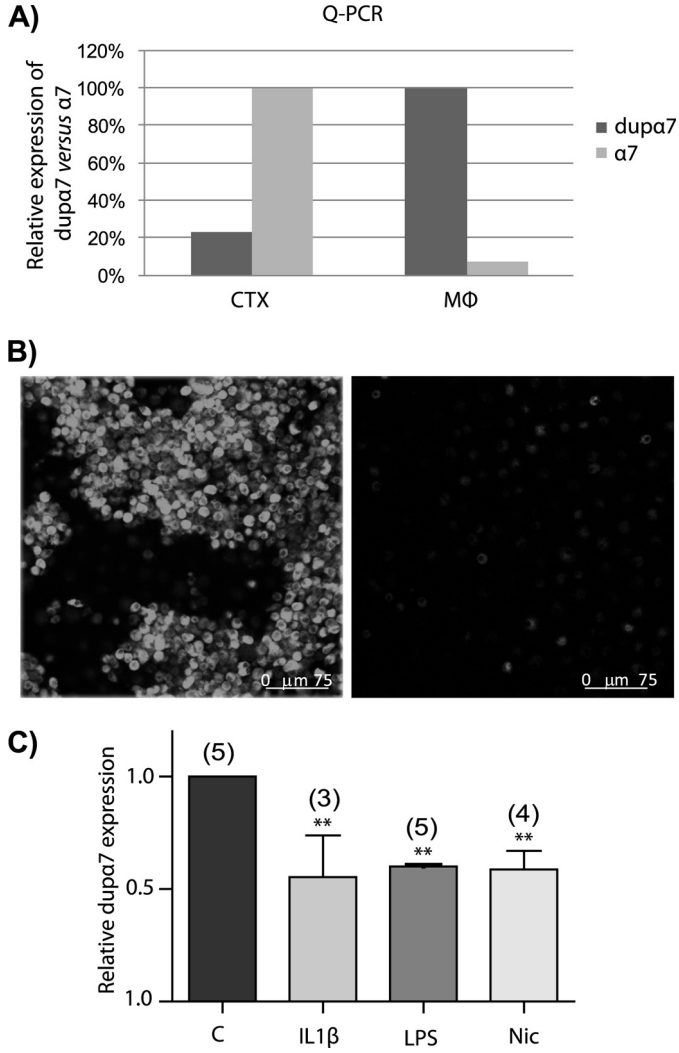

FIGURE 7. **Levels of dupα7 and α7 mRNA in different samples and regulation of dupα7 mRNA levels by different treatments.** *A*, relative expression levels of dupα7 *versus* α7 mRNA in CTX and MØ determined by Q-PCR; values were obtained in triplicate and correspond to a single CTX sample and two cultures of MØ from different donors. *B,* confocal images of MØ (out of five) in culture immunostained with FITC-αBgtx (*left panel*). Cells from the same culture preincubated with a high concentration (500 µM) of nicotine (*right panel*). *C,* effect of different treatments on the expression levels of dupα7 mRNA in cultured human MØ. Cells were incubated overnight with IL-1β (25 ng·ml^{-1}), LPS (100 ng·ml^{-1}), and nicotine (1 µM) or untreated. The *bars* show the mean ± S.E. of values, obtained in triplicate, and quantified by Q-PCR in the number of cultures from different healthy donors shown in *parentheses*. Data were analyzed by ANOVA and Dunnett post hoc tests. **, $p \leq 0.01$ with respect to control.

DISCUSSION

In this study we have cloned and expressed, for the first time, the full-length coding sequence of dupα7 in GH4C1 cells and oocytes. Additionally, we have performed a functional study of the protein expressed in the latter cell type. Our results indicate that dupα7 acted as a dominant negative regulator of α7 nAChR activity through a mechanism involving reduction in the number of functional α7 nAChRs incorporated into the oocyte surface. Determining whether the dupα7 subunit plays a functional role *in vivo*, wherever it is co-expressed with α7, requires additional experiments, but our preliminary results obtained in human cerebral cortex, human macrophages, and HL-60 cells suggest this possibility. Here, we discuss the most relevant results of this study.

The parallel confocal analysis of dupα7 and α7 protein expression in transfected GH4C1 cells and in mRNA-injected oocytes labeled with the Mab306 antibody indicates that the two cell types express both foreign proteins, although their patterns and expression levels differ. Thus, GH4C1 cells show a similar high α7 and dupα7 expression (Fig. 1, *A* and *C*), although a careful analysis of the α7 expression along the *x* axis of the cell reveals a peak localized in the cell membrane, although the dupα7 expression peak seems to have an inner location, probably within the ER (Fig. 1*B*). Meanwhile, expression levels of dupα7 on the cell surface of mRNA-injected oocytes represent only one-third of that of the α7 subunit (Fig. 2*B*), making it likely that most of the synthesized dupα7 proteins in oocytes are retained in the ER. However, our data do not preclude the possibility that a small fraction of dupα7 can form homo- or heteropentameric structures with other nAChR subunits able to migrate to the cell membrane.

Despite the low expression of dupα7 compared with α7 in the oocyte surface, there is no doubt that the first protein clearly interferes with the second. This assertion is deduced from electrophysiological records of I_{Nic} obtained in oocytes injected with different combinations of α7/dupα7 mRNA (Fig. 3, *A* and *B*). Thus, although dupα7 subunits are not capable of forming by themselves, homomeric nAChRs activated by ACh, or nicotine (not shown), they do produce a concentration-dependent dominant negative regulatory effect on α7 current. The question that now arises is to identify the mechanism through which dupα7 exerts this effect. The following hypotheses, individually or in combination, could provide an answer. Thus, dupα7 could do the following: 1) act at the transcriptional level of *CHRNA7*; 2) interfere with the proper oligomerization and assembly of α7 subunits in the ER, decreasing the number of mature α7 nAChRs able to migrate to the oocyte membrane; and/or 3) be integrated into a putative "α7/dupα7 heteromeric receptor" whose affinity or gating mechanism would be affected by the incorporation of the atypical subunit.

The first proposal can be ruled out, at least in terms of the dominant negative effect of dupα7 on α7 nAChRs in oocytes because, in this case, the injected mRNAs are obtained by *in vitro* transcription from the corresponding cDNAs. Although our results cannot rule out the possibility that dupα7 might produce some kind of interference *in vivo* at the transcriptional level of *CHRNA7*, this is unlikely because native transcripts that effectively regulate gene expression are "antisense" (44) and the orientation of the dupα7 transcript in human brain is in the "sense" direction of transcription (26).

Collectively, our data tend to support the second hypothesis because dupα7 co-expression significantly reduces the number of α7 nAChRs expressed on the oocyte surface, as can be inferred by the drastic decrease of fluorescent signal in Mab306-incubated oocytes as well as by the reduction of the B_{max} in ^{125}I-α Bgtx binding assays (Fig. 4). This hypothesis is further reinforced by the similar degree of reduction of both I_{Nic} (≈ 74%) and α7 nAChR expression (≈70%) in FITC-

αBgtx-labeled oocytes injected with equimolar amount of α7 and dupα7 mRNAs (Figs. 3*B* and 4*B, right panel*).

In relation to the third hypothesis, two of our findings seem to support this alternative in combination with the second proposal raised above. On the one hand, there was a small but statistically significant increase of K_d in oocytes co-injected with the combination 1:4 of α7/dupα7 mRNA compared with those injected with α7 mRNA alone (Fig. 4*C*, *bottom panel*). Because K_d is the reciprocal of affinity, the higher the K_d value, the lower the affinity of the receptor expressed by Bgtx. On the other hand, there was a different behavior of PNU120596 and 5HI in relation to their ability to enhance I_{ACh} in oocytes injected with different combinations of α7/dupα7 mRNA (Fig. 5). Although the former drug distinguishes between different groups of oocytes, the second does not. These results can be interpreted in light of different α7 modulation sites required by one or the other positive allosteric modulators, because PNU120596 interacts with transmembrane domains whereas 5HI requires the extracellular N-terminal domain of the α7 subunit (40, 45, 46). Thus, PNU120596 could act on homo- and heteromeric receptors, whereas 5HI would do so only on homomeric α7 nAChRs.

Northern blot analysis shows a band of a size of 3.9 kb in human CTX and HL-60 cells that most likely corresponds to the dupα7 transcript (Fig. 6*A*). This assumption is based on two facts as follows: 1) the HL-60 cells appear to express only dupα7 transcript (25); and 2) analysis of the NCBI EST data base provides a theoretical prediction of the size of dupα7 mRNA of 3600 bp. If we added the ~200 bp corresponding to the poly(A^+) tail to this value, there is a good correlation between the predicted and the experimental size of dupα7 mRNA found in this study. The possibility that the 3.9-kb band of CTX corresponds to an α7 isoform is very remote because we have not been able to find any isoform with this size in the literature or in the NCBI EST data base. In fact, the Northern blot for the CTX mRNA in our study shows additional bands that probably correspond to several α7 isoforms because their sizes are consistent with those found in SHY-5Y cells (47, 48). Additionally, the GenBank™ sequence NM_000746 gives a size of the transcript encoded by the *CHRNA7* gene of 3,351 bp, which could correspond to the band of 3.3 kb identified in our experiments. By identification of polysome-bound mRNAs, our results show, for the first time, that dupα7 mRNA is being translated in HL-60 cells (Fig. 6*B*), a process that has not been demonstrated before because of the unavailability of a selective antibody.

After demonstrating that dupα7 mRNA is translated and that the resulting protein behaves as a dominant negative of α7 nAChR activity in *vitro*, it is time to consider whether dupα7 could play a relevant functional role *in vivo* in those tissues and cell types that also express α7 nAChRs, such as the central nervous system (49–51) where presynaptic α7 nAChRs regulate the release of different neurotransmitters (1–4, 52). The same can be said of α7 nAChRs in MØ, which have an essential role in the cholinergic anti-inflammatory response (34, 53–56). However, to assume that dupα7 could behave as an endogenous modulator for α7 nAChR activity *in vivo*, it is essential that it meet two conditions as follows: (i) its mRNA levels must be high enough in respect to α7, and/or (ii) the expression levels of this messenger should, in turn, be susceptible to modulation by external stimuli that require greater or lesser α7 activity.

When we explored the first condition in human CTX and MØ using Q-PCR, we found that dupα7 mRNA levels in the former tissue come to about one-fifth of those of α7 (Fig. 7*A*). This result is consistent with previous data obtained in the human prefrontal cortex showing that expression of α7 mRNA is five times higher than that of dupα7 (21). The low proportion of dupα7 relative to that of α7 mRNA in CTX is functionally relevant in accordance with our data from I_{Nic} recorded in oocytes injected with the combination 5:1 of α7/dupα7 mRNA (Fig. 3, *A* and *B*).

A result opposite to that of CTX was obtained in MØ, which preferentially express dupα7 over the α7 transcript (Fig. 7*A*). Human PBMC and lymphocytes (25, 27, 57) and HL-60 cells (Fig. 6*A*) behave similarly. Despite the low expression level of α7 mRNA in MØ, there is no doubt that it is efficiently translated given the high number of functional α7 nAChRs detected in our experiments (Fig. 7*B*) as well as in previous studies (34). Thus, the question now is why, despite the high level of dupα7 mRNA in MØ, α7 nAChR expression is high in these cells. At this time we do not have a convincing answer, although different efficiencies in translation and/or proper folding of the α7 and dupα7 proteins could be underlying these results. Additional experiments are needed to explore these possibilities.

In relation to the second condition for dupα7 playing a modulatory role *in vivo*, our results in MØ show that mRNA levels are actually being regulated (Fig. 7*C*). This is an interesting finding because stimulation of α7 nAChR in macrophages induces a clear anti-inflammatory response secondary to decreased production of pro-inflammatory cytokines (34, 53, 56, 58). In this context, our results show that one of these cytokines, IL-1β, as well as LPS, is able to reduce dupα7 mRNA expression by half. In these conditions, pro-inflammatory cytokines would repress dupα7 expression and therefore increase the number of functional α7 nAChRs; the net output of this feedback loop would be the attenuation of the inflammatory response. Additionally, our findings that nicotine markedly reduces the expression levels of dupα7 mRNA in MØ (Fig. 7*C*) are in complete agreement with recent *in vivo* results showing a lower α7 transcript expression in PBMC from smokers than from nonsmokers (57). Further experiments are needed to learn whether cerebral dupα7 mRNA expression can be regulated by different stimuli, as occurs in MØ. However, it is interesting to note that the ratio of the α7/dupα7 transcripts varies in different brain regions as well as in individuals addicted to drugs or suffering certain psychiatric disorders. This is the case in schizophrenic patients, who show a general decrease in brain α7 mRNA and all *CHRNA7* transcription products that is most marked in the corpus callosum (26). The effect of nicotine in reducing dupα7 mRNA levels found in our study could explain, at least in part, the relief of symptoms experienced by these patients after smoking. Also, in bipolar disorder, an imbalance in the ratio of

CHRNA7/*CHRFAM7A* transcripts due to increased expression of dupα7 mRNA has been found (21).

In summary, our data are consistent with the idea that the product resulting from the partial duplication of the *CHRNA7* gene is likely to be modulated in a paracrine and endocrine manner, both in physiological as well as pathological situations, thereby exerting a negative modulating effect on α7 nAChR activity. Thus, previous findings regarding the *CHRFAM7A* and its possible association with psychiatric disorders can now be interpreted in the light of these new results.

Acknowledgments—We thank Prof. Henk Sipma (Johnson & Johnson Pharmaceutical Research and Development, Division of Janssen Pharmaceutica N. V, Beerse, Belgium) for donating the plasmids α7·pST64 and α7·pCDNA.3 and Prof. Millet Treining (Medical School, The Hebrew University of Jerusalem) for providing the plasmid hRIC3·pGEMH19. We also thank the Transfusion Center of the Comunidad de Madrid for providing the human buffy coats. We also thank Prof. J. Javier Sanchez (Department of Preventive Medicine and Public Health, Medical School, Universidad Autónoma de Madrid) for the advice in conducting statistical analysis.

REFERENCES

1. Li, D. P., Pan, Y. Z., and Pan, H. L. (2001) *Brain Res.* **920,** 151–158
2. Gray, R., Rajan, A. S., Radcliffe, K. A., Yakehiro, M., and Dani, J. A. (1996) *Nature* **383,** 713–716
3. Zhang, J., and Berg, D. K. (2007) *J. Physiol.* **579,** 753–763
4. Dickinson, J. A., Kew, J. N., and Wonnacott, S. (2008) *Mol. Pharmacol.* **74,** 348–359
5. Dajas-Bailador, F. A., Lima, P. A., and Wonnacott, S. (2000) *Neuropharmacology* **39,** 2799–2807
6. Mechawar, N., Saghatelyan, A., Grailhe, R., Scoriels, L., Gheusi, G., Gabellec, M. M., Lledo, P. M., and Changeux, J. P. (2004) *Proc. Natl. Acad. Sci. U.S.A.* **101,** 9822–9826
7. Shaw, S., Bencherif, M., and Marrero, M. B. (2002) *J. Biol. Chem.* **277,** 44920–44924
8. Freedman, R., Hall, M., Adler, L. E., and Leonard, S. (1995) *Biol. Psychiatry* **38,** 22–33
9. Guan, Z. Z., Zhang, X., Blennow, K., and Nordberg, A. (1999) *Neuroreport* **10,** 1779–1782
10. Dineley, K. T., Westerman, M., Bui, D., Bell, K., Ashe, K. H., and Sweatt, J. D. (2001) *J. Neurosci.* **21,** 4125–4133
11. Oddo, S., and LaFerla, F. M. (2006) *J. Physiol. Paris* **99,** 172–179
12. Shytle, R. D., Silver, A. A., Lukas, R. J., Newman, M. B., Sheehan, D. V., and Sanberg, P. R. (2002) *Mol. Psychiatry* **7,** 525–535
13. Arias, H. R., Richards, V. E., Ng, D., Ghafoori, M. E., Le, V., and Mousa, S. A. (2009) *Int. J. Biochem. Cell Biol.* **41,** 1441–1451
14. Rosas-Ballina, M., and Tracey, K. J. (2009) *Neuron* **64,** 28–32
15. Gault, J., Robinson, M., Berger, R., Drebing, C., Logel, J., Hopkins, J., Moore, T., Jacobs, S., Meriwether, J., Choi, M. J., Kim, E. J., Walton, K., Buiting, K., Davis, A., Breese, C., Freedman, R., and Leonard, S. (1998) *Genomics* **52,** 173–185
16. Riley, B., Williamson, M., Collier, D., Wilkie, H., and Makoff, A. (2002) *Genomics* **79,** 197–209
17. Gault, J., Hopkins, J., Berger, R., Drebing, C., Logel, J., Walton, C., Short, M., Vianzon, R., Olincy, A., Ross, R. G., Adler, L. E., Freedman, R., and Leonard, S. (2003) *Am. J. Med. Genet. B. Neuropsychiatr. Genet.* **123B,** 39–49
18. Locke, D. P., Archidiacono, N., Misceo, D., Cardone, M. F., Deschamps, S., Roe, B., Rocchi, M., and Eichler, E. E. (2003) *Genome Biol.* **4,** R50
19. Raux, G., Bonnet-Brilhault, F., Louchart, S., Houy, E., Gantier, R., Levillain, D., Allio, G., Haouzir, S., Petit, M., Martinez, M., Frebourg, T., Thibaut, F., and Campion, D. (2002) *Mol. Psychiatry* **7,** 1006–1011
20. Hong, C. J., Lai, I. C., Liou, L. L., and Tsai, S. J. (2004) *Neurosci. Lett.* **355,** 69–72
21. De Luca, V., Likhodi, O., Van Tol, H. H., Kennedy, J. L., and Wong, A. H. (2006) *Acta Psychiatr. Scand.* **114,** 211–215
22. Flomen, R. H., Collier, D. A., Osborne, S., Munro, J., Breen, G., St Clair, D., and Makoff, A. J. (2006) *Am. J. Med. Genet. B. Neuropsychiatr. Genet.* **141B,** 571–575
23. Fehér, A., Juhász, A., Rimanóczy, A., Csibri, E., Kálmán, J., and Janka, Z. (2009) *Dement. Geriatr. Cogn. Disord.* **28,** 56–62
24. Sinkus, M. L., Lee, M. J., Gault, J., Logel, J., Short, M., Freedman, R., Christian, S. L., Lyon, J., and Leonard, S. (2009) *Brain Res.* **1291,** 1–11
25. Villiger, Y., Szanto, I., Jaconi, S., Blanchet, C., Buisson, B., Krause, K. H., Bertrand, D., and Romand, J. A. (2002) *J. Neuroimmunol.* **126,** 86–98
26. Severance, E. G., and Yolken, R. H. (2008) *Genes Brain Behav.* **7,** 37–45
27. Perl, O., Strous, R. D., Dranikov, A., Chen, R., and Fuchs, S. (2006) *Neuropsychobiology* **53,** 88–93
28. van Maanen, M. A., Stoof, S. P., van der Zanden, E. P., de Jonge, W. J., Janssen, R. A., Fischer, D. F., Vandeghinste, N., Brys, R., Vervoordeldonk, M. J., and Tak, P. P. (2009) *Arthritis Rheum.* **60,** 1272–1281
29. Herrero, C. J., García-Palomero, E., Pintado, A. J., García, A. G., and Montiel, C. (1999) *Br. J. Pharmacol.* **127,** 1375–1387
30. Pintado, A. J., Herrero, C. J., García, A. G., and Montiel, C. (2000) *Br. J. Pharmacol.* **130,** 1893–1902
31. Solís-Garrido, L. M., Pintado, A. J., Andrés-Mateos, E., Figueroa, M., Matute, C., and Montiel, C. (2004) *J. Biol. Chem.* **279,** 52414–52424
32. Serantes, R., Arnalich, F., Figueroa, M., Salinas, M., Andrés-Mateos, E., Codoceo, R., Renart, J., Matute, C., Cavada, C., Cuadrado, A., and Montiel, C. (2006) *J. Biol. Chem.* **281,** 14632–14643
33. de Almeida, M. C., Silva, A. C., Barral, A., and Barral Netto, M. (2000) *Mem. Inst. Oswaldo Cruz* **95,** 221–223
34. Wang, H., Yu, M., Ochani, M., Amella, C. A., Tanovic, M., Susarla, S., Li, J. H., Wang, H., Yang, H., Ulloa, L., Al-Abed, Y., Czura, C. J., and Tracey, K. J. (2003) *Nature* **421,** 384–388
35. Herrero, C. J., Alés, E., Pintado, A. J., López, M. G., García-Palomero, E., Mahata, S. K., O'Connor, D. T., García, A. G., and Montiel, C. (2002) *J. Neurosci.* **22,** 377–388
36. García-Guzmán, M., Sala, F., Sala, S., Campos-Caro, A., and Criado, M. (1994) *Biochemistry* **33,** 15198–15203
37. del Prete, M. J., Vernal, R., Dolznig, H., Müllner, E. W., and Garcia-Sanz, J. A. (2007) *RNA* **13,** 414–421
38. Sweileh, W., Wenberg, K., Xu, J., Forsayeth, J., Hardy, S., and Loring, R. H. (2000) *Brain Res. Mol. Brain Res.* **75,** 293–302
39. Balduzzi, R., Cupello, A., Diaspro, A., Ramoino, P., and Robello, M. (2001) *Biochim. Biophys. Acta* **1539,** 93–100
40. Zwart, R., De Filippi, G., Broad, L. M., McPhie, G. I., Pearson, K. H., Baldwinson, T., and Sher, E. (2002) *Neuropharmacology* **43,** 374–384
41. Grønlien, J. H., Håkerud, M., Ween, H., Thorin-Hagene, K., Briggs, C. A., Gopalakrishnan, M., and Malysz, J. (2007) *Mol. Pharmacol.* **72,** 715–724
42. Pradet-Balade, B., Boulmé, F., Beug, H., Müllner, E. W., and Garcia-Sanz, J. A. (2001) *Trends Biochem. Sci.* **26,** 225–229
43. Pradet-Balade, B., Boulmé, F., Müllner, E. W., and Garcia-Sanz, J. A. (2001) *BioTechniques* **30,** 1352–1357
44. Osato, N., Suzuki, Y., Ikeo, K., and Gojobori, T. (2007) *Genetics* **176,** 1299–1306
45. Young, G. T., Zwart, R., Walker, A. S., Sher, E., and Millar, N. S. (2008) *Proc. Natl. Acad. Sci. U.S.A.* **105,** 14686–14691
46. Bertrand, D., Bertrand, S., Cassar, S., Gubbins, E., Li, J., and Gopalakrishnan, M. (2008) *Mol. Pharmacol.* **74,** 1407–1416
47. Peng, X., Katz, M., Gerzanich, V., Anand, R., and Lindstrom, J. (1994) *Mol. Pharmacol.* **45,** 546–554
48. Groot Kormelink, P. J., and Luyten, W. H. (1997) *FEBS Lett.* **400,** 309–314
49. Chen, D., and Patrick, J. W. (1997) *J. Biol. Chem.* **272,** 24024–24029
50. Court, J. A., Martin-Ruiz, C., Graham, A., and Perry, E. (2000) *J. Chem. Neuroanat.* **20,** 281–298
51. Drisdel, R. C., and Green, W. N. (2000) *J. Neurosci.* **20,** 133–139
52. Sharma, G., and Vijayaraghavan, S. (2008) *Curr. Med. Chem.* **15,**

2921–2932
53. Borovikova, L. V., Ivanova, S., Zhang, M., Yang, H., Botchkina, G. I., Watkins, L. R., Wang, H., Abumrad, N., Eaton, J. W., and Tracey, K. J. (2000) *Nature* **405,** 458–462
54. de Jonge, W. J., van der Zanden, E. P., The, F. O., Bijlsma, M. F., van Westerloo, D. J., Bennink, R. J., Berthoud, H. R., Uematsu, S., Akira, S., van den Wijngaard, R. M., and Boeckxstaens, G. E. (2005) *Nat. Immunol.* **6,** 844–851
55. Pavlov, V. A., and Tracey, K. J. (2006) *Biochem. Soc. Trans.* **34,** 1037–1040
56. van Westerloo, D. J., Giebelen, I. A., Florquin, S., Bruno, M. J., Larosa, G. J., Ulloa, L., Tracey, K. J., and van der Poll, T. (2006) *Gastroenterology* **130,** 1822–1830
57. Severance, E. G., Dickerson, F. B., Stallings, C. R., Origoni, A. E., Sullens, A., Monson, E. T., and Yolken, R. H. (2009) *J. Neural. Transm.* **116,** 213–220
58. Wang, H., Liao, H., Ochani, M., Justiniani, M., Lin, X., Yang, L., Al-Abed, Y., Wang, H., Metz, C., Miller, E. J., Tracey, K. J., and Ulloa, L. (2004) *Nat. Med.* **10,** 1216–1221